ELSEVIER

Biochimica et Biophysica Acta 1565 (2002) 81–90

BIOCHIMICA ET BIOPHYSICA ACTA
BBA

www.bba-direct.com

Long-range effects on the binding of the influenza HA to receptors are mediated by changes in the stability of a metastable HA conformation

Dalit Shental-Bechor [a], Tsafi Danieli [b], Yoav I. Henis [b], Nir Ben-Tal [a,*]

[a] *Department of Biochemistry, George S. Wise Faculty of Life Sciences, Tel Aviv University, Ramat Aviv 69978, Israel*
[b] *Department of Neurobiochemistry, George S. Wise Faculty of Life Sciences, Tel Aviv University, Ramat Aviv 69978, Israel*

Received 25 February 2002; received in revised form 19 June 2002; accepted 10 July 2002

Abstract

X-ray studies show that influenza hemagglutinin (HA) forms an elongated structure connecting the influenza virus at one end to cell-surface receptors at the other. At neutral pH, the 20 N-terminal residues of HA2—referred to as the fusion peptide—are buried in a hydrophobic pocket, about 100 Å away from the receptor-binding site, and thus seem unlikely to affect HA binding to the receptor. To test this assumption, we mutated residues in the fusion peptide, heterologically expressed the mutated proteins in COS7 cells, and examined their ability to bind fluorescently labeled red blood cells (RBCs). Surprisingly, a significantly reduced binding was recorded for some of the mutants. Ample experimental data indicate that HA has at least two forms: the native structure at neutral pH (N) that is metastable and the fusogenic form (F), observed at low pH, which is stable. Thus, a simple interpretation of our data is that HA can bind to its receptors at the RBC surface in the N form much more effectively than in the F (or in any other stable) form and that the altered binding properties are due to destabilizing effects of the mutations on the N form. That is, some of the mutations involve reduction in the free energy barrier between the N and F forms. This, in turn, leads to reduction in the population of the N form, which is the only form capable of binding to the cell-surface receptors. To explore this possibility, we estimated the stability free energy difference between HA wild-type (wt) and mutants in the N form using an empirical surface tension coefficient. The calculated stability differences correlated well with the measured binding, supporting the above interpretation. Our results are examined taking into account the available experimental data on the affinity of different soluble and membrane-attached forms of HA to its receptors.

Keywords: Hemagglutinin; Cell-surface receptor; Fusion peptide; Protein binding and stability; Mutagenesis; Fluorescent microscopy; Continuum solvent model

1. Introduction

Infection of animal cells by the influenza virus begins with binding of the virus via its hemagglutinin (HA) protein to sialic acid residues, present in membrane proteins and lipids. The bound virion is then internalized into endosomes by receptor-mediated endocytosis. Ultimately, the viral envelope fuses with the mature endosomal membrane after the HA protein becomes fusogenic in response to a drop in pH [1–6]. The HA from the X:31 strain is produced as a 550-residue-long precursor, called HA0, which is proteolytically cleaved into two subunits: HA1 (residues 1–328 of HA0) and HA2 (residues 330–550). HA1 and HA2 are covalently bonded by a disulfide bond.

HA has been studied intensively using molecular biology, biochemical and biophysical methods. The site that binds to the sialic acid-containing receptors was identified on the HA1 subunit, and a hydrophobic segment containing the first 20 residues of HA2 was shown to be involved in membrane fusion and was termed "the fusion peptide." The X-ray crystal structure of HA has been determined in three different forms: (a) the HA0 precursor [7], (b) at neutral pH when it binds the sialic acid receptor [8,9], and (c) prior to membrane fusion—in the acidic pH of the mature endosome [10]. We focus on the binding of HA to the receptor and therefore on its structure at neutral pH (Fig. 1). HA has a long stem structure of about 135 Å, oriented roughly perpendicular to the virus membrane and bridging the virus with the host cell plasma membrane. HA is a homotrimer

* Corresponding author. Tel.: +972-3-6496709; fax: 972-3-6406834.
E-mail address: bental@ashtoret.tau.ac.il (N. Ben-Tal).
URL: http://www.ashtoret.tau.ac.il.

0005-2736/02/$ - see front matter © 2002 Elsevier Science B.V. All rights reserved.
PII: S0005-2736(02)00511-4

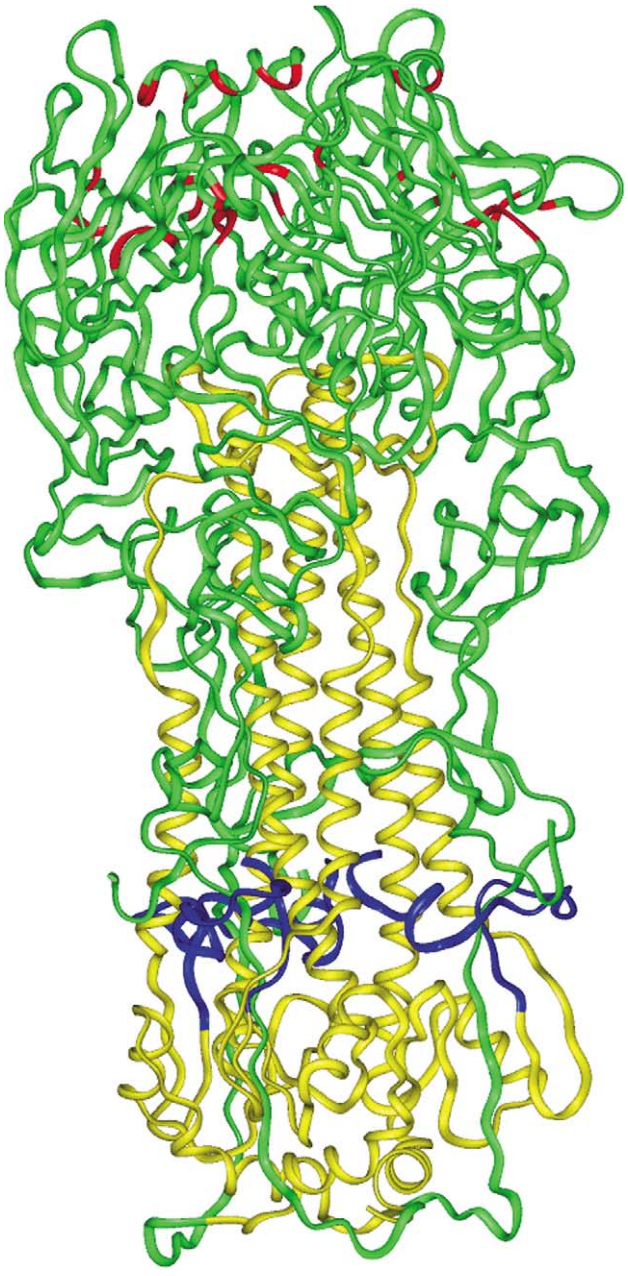

Fig. 1. A ribbon diagram of influenza HA in its (metastable) conformation at neutral pH, referred to as the "N" form. The elongated stem structure connects the virus at the bottom end to the membrane of the host cell at the top end. The HA1 and HA2 subunits are colored in green and yellow, respectively. Residues Tyr98, Trp153, His183, Glu190, Leu194, Cys97, Pro99, Cys139, Pro147, Tyr195 and Arg229 of HA1 comprise the sialic acid binding site and are colored red. They are located about 100 Å from the 20 residues of the "fusion peptide" at the N-terminus of HA2 (blue).

comprised of an elongated coiled-coil (~ 80 Å) with a globular domain at the top. Three long α-helices of HA2 (Fig. 1, yellow), each from a different monomer, form the coiled-coil structure. The globular domain contains a part of HA1 of each monomer (Fig. 1, green) and includes three receptor-binding sites, marked in red. The fusion peptide, marked in blue, is located about 100 Å away from the sialic acid binding site.

In the process of studies aimed at identifying residues that are crucial for membrane fusion, we mutated residues in the HA fusion peptide. Since binding of the virus to the target cell is a pre-requisite for fusion, we expressed the HA mutants in COS7 cells and examined their ability to confer binding of red blood cells (RBCs) to the HA-expressing cells. Surprisingly, although the mutations are about 100 Å away from the binding site, some of them significantly altered the ability of the HA-expressing cells to bind RBCs. The results of the mutagenesis study are reported below together with calculations to support an explanation of this observation.

At least two conformations were detected for the mature HA molecule [11]. The first was obtained at neutral pH [8] and is usually referred to as the native structure (N). The second was obtained at acidic pH [10], and is referred to as the fusogenic structure (F) because of its fusogenic capacity. The available experimental data indicate that F is stable while N is only metastable [1,12–14] (reviewed in Ref. [3]). That is, the free energy of the N form, G_N, is higher than the free energy of the F form, G_F. The conformational change that occurs after a pH drop switches the HA protein from the metastable form N to the stable form F through the partially denatured form D, whose free energy is G_D (Fig. 2a). The free energy difference $G_D - G_N$ is the height of the kinetic barrier governing the transformation. This energy barrier is a measure of the stability of the N form; the higher it is, the more stable the N form is. Our working hypothesis, presented in the thermodynamic cycle of Fig. 2B, is that the binding level of HA to its cell-surface receptors is influenced by the stability of the metastable form N. In other words, for some mutants, the free energy barrier $G_D - G_N$ is reduced compared to that of the wt, rendering these mutants less stable than the wt. This may result in HA switching conformation from N to another conformation, such as F, which may be more stable but with less capacity to bind to cell-surface receptors. In this respect, it is noteworthy that in the absence of a target membrane, exposure of virions or cells expressing HA to low pH, presumably involving the shift of HA from the N to the F form, was shown to inactivate the fusion activity of HA of some influenza subtypes, including the X:31 strain used here, and to reduce its lateral mobility in the membrane [15–18].

To calculate the height of the free energy barrier $G_D - G_N$ of each mutant relative to the wt, we need the structures of the wt and each mutant at the N and D forms. We assume that the structures of the HA mutants (single or double mutations) in the N conformation are fairly similar to the known structure of the wt HA. However, we do not know the structure of neither the wt nor the mutants in the D form. Therefore, we assume that during the conformational change from N to F, the HA protein undergoes denaturation which is limited to the fusion peptide site. In the calculations, we approximate the structure of the denatured fusion

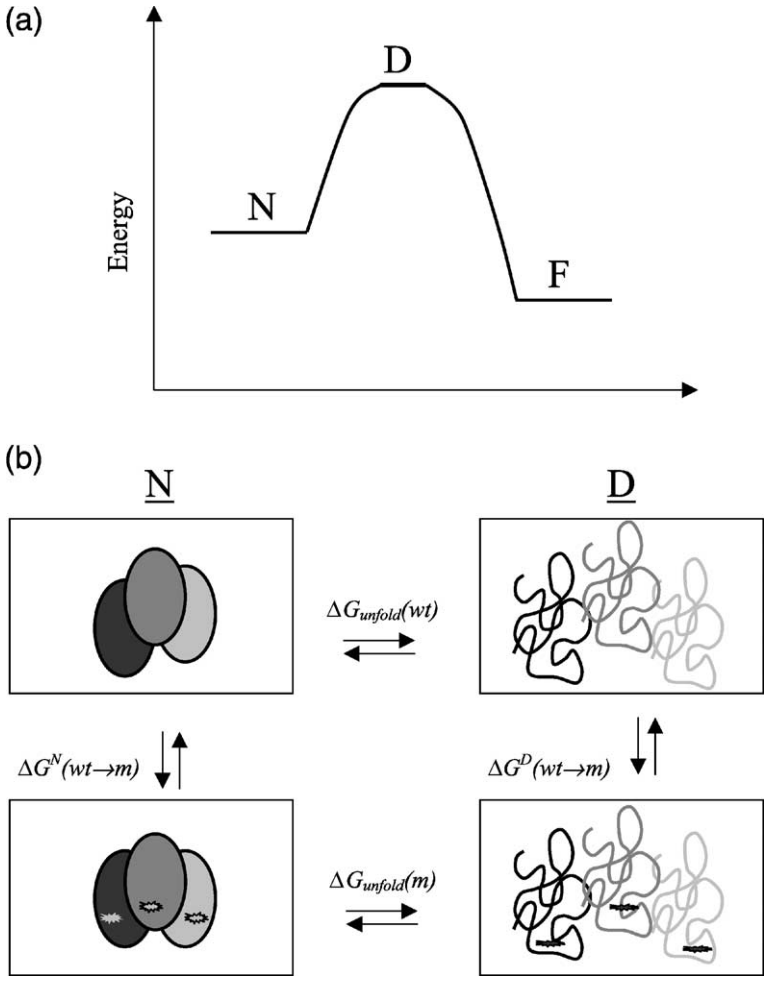

Fig. 2. (a) The relative free energy of HA along a hypothetical path from the native form (at neutral pH) "N", through the partially denatured form "D", to the fusogenic form (at acidic pH) "F". The scheme illustrates the metastable nature of the N form. (b) Thermodynamic cycle relating the stability of wild-type (wt) and mutant HA trimers in the metastable native-state N (solid shapes) to their partially denatured state D (scribbled line). The HA mutants are represented by the additional black spots. $\Delta G_{\mathrm{unfold}}(\mathrm{wt})$ and $\Delta G_{\mathrm{unfold}}(\mathrm{m})$ are the unfolding free energies of wild-type and mutant HA. Our assumption is that the capacity of HA to bind to cell-surface receptors is effected by the stability of the molecule in the metastable form N, i.e., by the free energy of HA in its D and N forms, which corresponds to the barrier height in (a). Thus, the measured binding differences between mutant and wild-type HA, $\Delta\Delta G_{\mathrm{bind}}$, are related to their stability differences, $\Delta\Delta G_{\mathrm{stab}}$. That is, $\Delta\Delta G_{\mathrm{bind}} \approx \Delta\Delta G_{\mathrm{stab}} \equiv \Delta G_{\mathrm{unfold}}(\mathrm{wt}) - \Delta G_{\mathrm{unfold}}(\mathrm{m})$. It is evident from the thermodynamic cycle that $\Delta\Delta G_{\mathrm{stab}} = \Delta G^{\mathrm{N}}(\mathrm{wt} \rightarrow \mathrm{m}) - \Delta G^{\mathrm{D}}(\mathrm{wt} \rightarrow \mathrm{m})$, where $\Delta G^{\mathrm{N}}(\mathrm{wt} \rightarrow \mathrm{m})$ is the free energy difference between mutant and wild-type HA in their N forms and $\Delta G^{\mathrm{D}}(\mathrm{wt} \rightarrow \mathrm{m})$ is the free energy difference between mutant and wild-type HA in their D forms.

peptide (wt and mutants) as an extended conformation. Further, we assume that the dominant contribution to the stability free energy is from the nonpolar contributions to the solvation free energy, that comprise van der Waals' and solvent structure effects which together define the classic hydrophobic effect. Thus, we built the structure of each mutant by modifying residues in the known X-ray structure of HA wt (in the N form) and estimated the nonpolar solvation contributions to the stability free energy of each mutant relative to the wt by calculating the difference in the accessibility of each HA to the solvent. Despite the crude model, the method successfully reproduced the experimental data, supporting the assumption that reduced stability of the metastable N conformation shifts the HA population towards a conformation with higher stability but reduced receptor-binding capability.

2. Theory

The thermodynamic cycle of Fig. 2b introduces a simple interpretation of the experimental data. It assumes that HA binds to sialic acid-containing receptors only in its native conformation at neutral pH (N), which is metastable as mentioned above. HA mutants and wt in their N conformation have approximately identical affinities to sialic acid residues, and the difference in binding results from stability differences between mutants and wild-type. This occurs because destabilization of the N form shifts HA molecules to more stable but binding-incompetent conformations such as F. In the following, we present a simple approach for estimating the stability differences.

Protein stability is related to the unfolding free energy, defined as the free energy difference between the protein in

its unfolded and folded forms. The unfolding free energy includes many covalent and noncovalent terms, and it is a very difficult—usually impossible—task to calculate it from first principles. However, the relative stability of a protein mutant

$$\Delta\Delta G_{\mathrm{stab}} \equiv \Delta G_{\mathrm{unfold}}(\mathrm{wt}) - \Delta G_{\mathrm{unfold}}(\mathrm{m}) = \Delta G^{\mathrm{N}}(\mathrm{wt} \rightarrow \mathrm{m}) - \Delta G^{\mathrm{D}}(\mathrm{wt} \rightarrow \mathrm{m}) \quad (1)$$

is easier to estimate because of the high similarity between the wild-type and mutant proteins. For example, the covalent bonds of the wild-type and the mutants are usually virtually identical and therefore it is not necessary to consider them. Thus, one is typically left only with noncovalent contributions, such as hydrogen bonding, salt bridge formation, solvation free energy and contributions from residue confinement effects. The general view is that the main contribution to the relative stability of proteins comes from the solvation free energy [19–26]. We take this view to the extreme, assuming that the unfolding free energy difference between a mutant and wild-type protein in their native forms ($\Delta G^{\mathrm{N}}(\mathrm{wt} \rightarrow \mathrm{m})$) and in their unfolded forms ($\Delta G^{\mathrm{D}}(\mathrm{wt} \rightarrow \mathrm{m})$) can be approximated by the nonpolar contributions to the solvation free energy alone, neglecting all the other free energy components. Thus, denoting the nonpolar contributions to the solvation free energy of the mutant and wild-type protein by $G^{\mathrm{N-np}}(\mathrm{m})$ and $G^{\mathrm{N-np}}(\mathrm{wt})$, we get

$$\Delta G^{\mathrm{N}}(\mathrm{wt} \rightarrow \mathrm{m}) \equiv G^{\mathrm{N}}(\mathrm{m}) - G^{\mathrm{N}}(\mathrm{wt}) \approx G^{\mathrm{N-np}}(\mathrm{m}) - G^{\mathrm{N-np}}(\mathrm{wt}) \quad (2)$$

and an analogue expression for $\Delta G^{\mathrm{D}}(\mathrm{wt} \rightarrow \mathrm{m})$.

The nonpolar contribution to the solvation free energy has entropic origin and is assumed to be proportional to the water accessible surface area of the molecule [27]. Thus, $\Delta G^{\mathrm{N}}(\mathrm{wt} \rightarrow \mathrm{m})$ is given by the expression

$$\Delta G^{\mathrm{N}}(\mathrm{wt} \rightarrow \mathrm{m}) \approx \gamma(S^{\mathrm{N}}(\mathrm{m}) - S^{\mathrm{N}}(\mathrm{wt})) \quad (3)$$

where $S^{\mathrm{N}}(\mathrm{m})$ and $S^{\mathrm{N}}(\mathrm{wt})$ are the water accessible surface areas of the mutant and wild-type in their native state, and γ is a surface area proportionality constant (commonly referred to as a surface tension). Eq. (3) and its equivalent for the mutant and wild-type proteins in their unfolded forms are the key equations in this study and we used them to estimate the relative stability of each mutant with respect to HA wt. Typical γ values are in the range 0.02–0.05 kcal/(mol·Å^2) [20]. As we discuss further below, the exact value of γ does not matter for the purpose of this work, and we used $\gamma = 0.0278$ kcal/(mol·Å^2), a value that has been derived from the partitioning of alkanes between liquid alkane and water [28].

Obviously HA mutants that involve the replacement of large residues with small ones yield a decrease in the accessible surface area of the denatured form, i.e., $S^{\mathrm{D}}(\mathrm{m}) < S^{\mathrm{D}}(\mathrm{wt})$. Thus, they lead to negative $\Delta G^{\mathrm{D}}(\mathrm{wt} \rightarrow \mathrm{m})$ values. In contrast, the value of $\Delta G^{\mathrm{N}}(\mathrm{wt} \rightarrow \mathrm{m})$ of such mutants is context-dependent. If the residue is solvent-exposed, the replacement leads to negative $\Delta G^{\mathrm{N}}(\mathrm{wt} \rightarrow \mathrm{m})$ values. In such a case, $\Delta\Delta G_{\mathrm{stab}}$ of Eq. (1) will be small, i.e., the HA mutant and wt will be approximately equally stable in the N state and their cell-surface binding capacity will be similar. However, HA mutants involving the replacement of large buried residues with small ones, yield an increase in the accessible surface area, i.e., $S^{\mathrm{N}}(\mathrm{m}) > S^{\mathrm{N}}(\mathrm{wt})$, because a water cavity is formed in our model of the protein structure. In such a case, $\Delta\Delta G_{\mathrm{stab}}$ will be large, leading to reduced cell-surface binding of the HA mutant compared to wt. In reality, the structure of the mutant HA is likely to relax and close the cavity. Thus, our estimate of the magnitude of $\Delta G^{\mathrm{N}}(\mathrm{wt} \rightarrow \mathrm{m})$ is an upper bound for the real value. Likewise, our approximation of the denatured form as extended conformation maximizes the magnitude of its contribution. Thus, $\Delta G^{\mathrm{D}}(\mathrm{wt} \rightarrow \mathrm{m})$ is also an upper bound to the real value.

Eq. (3) implies that protein stability is linearly proportional to the water accessible surface area and that large globular proteins are therefore more stable than small ones. This is not necessarily true; Eq. (3) may be useful for estimating the relative stability of mutants, but is unlikely to hold for the comparison of two different proteins.

3. Materials and methods

3.1. Computational methods

The main problem in estimating mutation effects on protein stability is that changes corresponding to several kcal/mol or less are the result of large opposing contributions that nearly balance each other. To avoid this problem we relied, in essence, on the known X-ray crystal structure of HA and used Eqs. (1) and (3) to calculate the main contributions to protein stability, i.e., the solvation free energy. We also limited our analysis to the vicinity of the fusion peptide.

3.1.1. Structure of the wild-type

The X-ray crystal structure of the HA trimer–sialic acid complex was taken from entry number 1HGF in the PDB (http://www.rcsb.org/pdb/). Several sugar and water molecules have been observed in the crystal structure. They are scattered on the surface of the protein and we omitted them from the calculations since none of them were in direct contact with the binding site or the fusion peptide. Hydrogen atoms were added to the crystal structure using the molecular modelling set of tools in Insight97/Biopolymer (MSI, San Diego, CA, USA). The structure was then energy-minimized, using 200 steepest descent iterations and the cuff forcefield with a dielectric constant of 20 in order to adjust the molecule to the forcefield. The minimi-

zation had very little effect on the structure and the heavy-atoms RMS deviation between the minimized and non-minimized structures is only 0.2 Å.

3.1.2. Structures of mutants

Three-dimensional models of the mutants were built by altering residues in the minimized structure of the wild-type HA using Insight97/Biopolymer. The amino acids in a sphere of radius 15 Å around the geometric center of each mutated residue were then energy-minimized. Again, the minimization had a very limited effect and the heavy-atoms RMS deviations between the wild-type and each of the mutants never exceed 0.07 Å.

3.1.3. The denatured form

The denatured form was approximated as an extended state and we used Insight97/Biopolymer to build tripeptides corresponding to mutated residues and their nearest neighbors. Two models were built for each case; one with the wild-type residue and one with the mutant.

3.1.4. Nonpolar solvation free-energy calculations

The computation of the nonpolar contribution to the free energy is based on the difference between the water accessible surface area of the wild-type and mutant proteins (Eq. (3)). The total area of the wild-type and each of the mutants accessible to water was calculated using SurfV [29] (a computer program based on a modified Shrake and Rupley algorithm [30]), a water probe radius of 1.4 Å, and the atomic radii of the PARSE set of solvation parameters [28]. Only residues located within a radius of 7 Å from the geometrical center of each mutated residue were included in these calculations to reduce the error.

3.2. Experimental methods

3.2.1. HA mutants

HA mutants were generated by site-directed mutagenesis [31] on single-stranded phagemids of pSM-HA [32] (an SV40 phagemid containing the full-length X:31 HA cDNA). The vector was used as a single-stranded bacteriophage for mutagenesis and as a vector for transient expression under SV40 promoter. All mutants were verified by sequence analysis.

3.2.2. Transfections

COS7 cells in 60 mm dishes were transiently transfected with 3 μg DNA of each HA mutant in pSM, using Transfectam™ (Promega). After 24 h, the cells in each dish were replated into two 60 mm dishes. One dish served for measuring RBC binding, and the other for determination of HA surface expression level by biotinylation (see below). This protocol ensures that the surface HA level is measured for the same transfected dish used for the binding assay. Forty-eight hours later, the cells were treated with neuraminidase (0.2 mg/ml) and TPCK-trypsin (10 μg/ml; Sigma) as described in Ref. [33] to cleave cell-surface HA0 to S–S linked HA1/HA2, and taken for surface biotinylation and RBC binding experiments.

3.2.3. Determination of cell-surface levels of HA mutants by surface biotinylation

The 60 mm dishes with the HA-expressing COS7 cells described above were chilled and treated with the membrane-impermeable biotinylating reagent sulfosuccinimidyl-6-(biotinamido) hexanoate (NHS-LC-Biotin; Pierce) as described in Ref. [34]. The cells were lysed

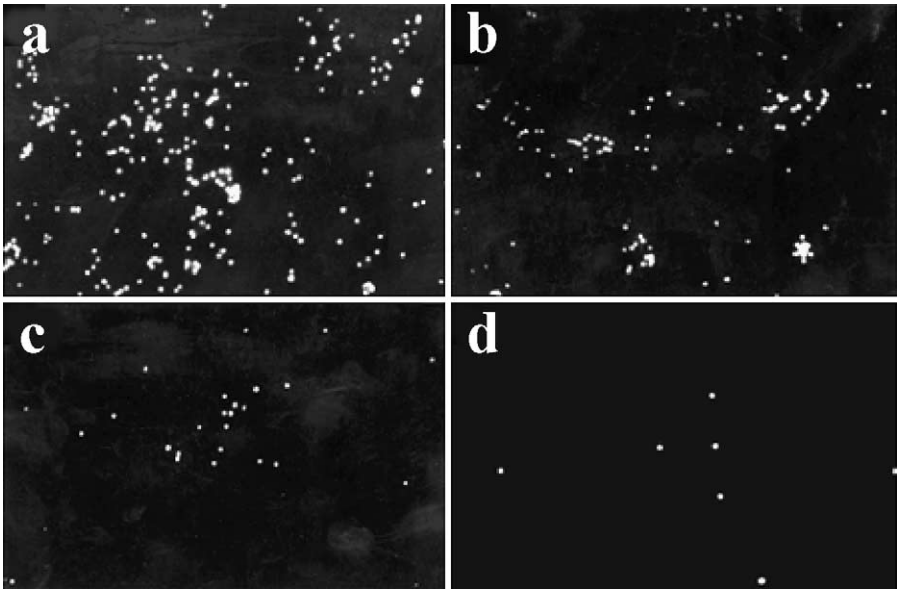

Fig. 3. Representative fluorescence micrographs of R18-RBCs bound to COS7 cells expressing different HA mutants. R18-RBCs were bound to COS7 cells expressing various HA mutants as described in Experimental methods. (a) I6Q (+++), (b) I10N_N12I (++−), (c) W14Q (+/−), (d) W14S (+−−).

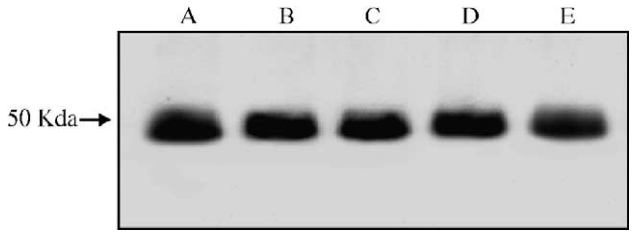

Fig. 4. Cell-surface expression of representative HA mutants. COS7 cells expressing HA wt and representative mutants were transfected in parallel. The cells in each dish were split into 60 mm (for binding studies) and 30 mm (for surface HA level determination) dishes, and the latter were labeled with membrane-impermeable NHS-LC-Biotin as described in Experimental methods. After immunoprecipitation with anti-HA, SDS-PAGE and blotting, biotinylated HA was visualized by labeling with streptavidin-HRP and ECL (see Experimental methods). (A) I6Q, (B) I10N_N12I, (C) W14Q, (D) W14S, (E) HA wt. All the HAs exhibited similar expression levels on the cell surface; RBC binding studies employed transfected samples where the variations in HA surface expression levels did not exceed 10%.

in 0.5 ml lysis buffer (50 mM Hepes pH 7.5, 1% NP-40, containing 1 mM PMSF, 2 μg/ml leupeptin, 4 μg/ml aprotinin, and 0.5 mM iodoacetamide), spun in a microfuge to remove insoluble material, and immunoprecipitated with 2 μg/ml of HC3 mouse monoclonal IgG [35] (a gift from Dr. J.J. Skehel) as described in Ref. [34]. After precipitation using protein A-agarose, the immunocomplexes were washed three times with wash buffer (20 mM Hepes, 130 mM NaCl and 1% NP40). The pellets were suspended in 40 μl of Laemmli loading buffer (containing SDS and mercaptoethanol), boiled 5 min, and subjected to SDS-PAGE on 10% acrylamide gels. The proteins were electroblotted onto nitrocellulose membranes, and the biotinylated proteins were identified by labeling with streptavidin-HRP (Pierce) (1 μg/ml, 1 h, 4 °C) and ECL (Amersham) as described in Ref. [36]. Densitometry was performed on a BioImaging System 202D (Dynco-Renium) using TINA 2.0 software (Ray Test).

3.2.4. Binding of R18-RBCs to HA-expressing cells

Freshly drawn RBCs were labeled with the fluorescent lipid probe octadecylrhodamine B chloride (R18; Molecular Probes) as described in Ref. [33]. The R18-RBCs were suspended in RPMI medium (Biological Industries, Beth Haemek) supplemented with 50 mM Hepes (pH 7.4), stored at 4 °C and used within 4 days. For binding to HA-expressing COS7 cells, each 60 mm dish was incubated with 2 ml of 0.05% hematocrit of R18-RBCs in the RPMI/Hepes medium (20 min, 25 °C) and washed three times. The binding levels were evaluated by counting the number of R18-RBCs bound to 200 cells in each sample under a fluorescence microscope with rhodamine filters. We employed a binding index relative to HA wt (which was always measured in parallel and was taken as 100%): (+++) indicates R18-RBC binding level similar (± 10%) to that of HA wt; (++−) stands for ~ 70% binding; (+/−) indicates ~ 40% binding; and (+−−) stands for 5% binding or less relative to HA wt.

4. Results

4.1. Experimental results on RBC binding to HA-expressing COS7 cells

A series of mutants (13 single and 3 double mutations) in the fusion peptide region of X:31 HA were prepared as described in Experimental methods (Table 1). Each mutant was transiently expressed in COS7 cells, and their ability to bind fluorescent-labeled RBCs (Fig. 3, Table 1) was measured. When comparing the levels of RBC binding to cells expressing different HA mutants, it was important to eliminate the possible contribution of variations in the surface expression levels of the different mutants. Such variations may arise due to differences in transfection efficiency and in transport of the different mutants to the cell surface. There-

Table 1
The experimentally measured RBCs-binding and calculated stability of the HA mutants in the metastable N state (Fig. 2a) compared to wt

Mutant[a]	Calculated stability				Measured binding[b]
	$\Delta G^{D}_{(wt \rightarrow m)}$[c] (kcal/mol)	$\Delta G^{N}_{(wt \rightarrow m)}$[d] (kcal/mol)	$\Delta\Delta G_{stab}$[e] (kcal/mol)	Estimated binding[f]	
I6Y	3.7	−0.4	−4.1	(+++)	(+++)
F3Y_F9Y	2.2	−0.9	−3.1	(+++)	(+++)
F9Y	1.1	−0.3	−1.4	(+++)	(+++)
I6Q	−0.1	−0.4	−0.3	(+++)	(+++)
I18Q_F24Y	1.1	1.1	0.0	(+++)	(+++)
L2Q	−0.7	−0.5	0.2	(+++)	(+++)
I10Q	−0.1	0.8	0.8	(+++)	(+++)
I18Q	−0.1	1.4	1.5	(++−)	(+++)
W14Y	−2.3	−0.1	2.2	(++−)	(+++)
W14F	−3.5	−0.3	3.2	(++−)	(+++)
I10N	−2.6	1.0	3.6	(++−)	(+++)
I10N_N12I	−0.5	0.4	1.0	(++−)	(++−)
W14M	−5.1	1.0	6.2	(+/−)	(+/−)
W14Q	−6.6	1.5	8.2	(+/−)	(+/−)
W14S	−11.5	3.3	14.8	(+−−)	(+−−)
W14A	−12.4	4.0	16.4	(+−−)	(+−−)

[a] The list of mutations in single-letter amino acid symbols. The numbers relate to the location in the fusion peptide, starting with 1 at position 347. For example, I6Y is a mutant where Ile6 was replaced by Tyr, and F3Y_F9Y is a double mutant (at positions 3 and 9).

[b] The measured RBCs-binding index divided into four groups: (+++) indicates binding similar to the wild-type, (++−) indicates binding at about 70% of wild-type, (+/−) indicates binding at about 40% of wild-type and (+−−) binding at about 5%.

[c] Relative stability of mutant and wild-type HA in the denatured forms. The value reported is for a trimer, i.e., three times the calculated value per monomer.

[d] Relative stability of mutant and wild-type HA in the (metastable) folded trimeric forms.

[e] The stability free energy difference between wild-type and mutant HA, Eq. (1).

[f] An arbitrary conversion of the calculated relative stability into binding index (see text for details).

fore, for each set of comparative experiments performed on the same day, we used the same transfection buffer mix, the same suspension of fluorescent-labeled RBCs for the binding assay, and always included a sample transfected with HA wt as an "internal reference" (taken as 100% binding). Most importantly, the amounts of each mutant at the cell surface (which reflects a combination of both transfection efficiency and arrival at the cell surface) were measured on samples taken from each transfected dish by labeling cell-surface proteins with a membrane-impermeable biotinylation reagent, followed by immunoprecipitation of HA and Western blotting (see Experimental methods). Fig. 4 depicts a representative example of one set of such experiments. In general, the surface expression levels of all the mutants studied here were very close; the RBC binding studies employed transfected samples where the variations in HA surface expression levels did not exceed 10%.

The results of the RBC binding studies are summarized in Table 1. The various HA mutants fell into four major groups. Cells expressing the mutants I6Y, F3Y_F9Y, F9Y, I6Q, I18Q_F24Y, L2Q, I10Q, I18Q, W14Y, W14F and I10N bound the same amount of RBCs as HA wt (designated +++). The RBC binding capability of the I10N_N12I mutant was somewhat less than that of HA wt (~ 70%, designated ++−). The amount of RBCs bound by the W14M and W14Q mutants was ~ 40% of that bound by HA wt (+/−). Finally, two mutants (W14S and W14A) showed very low RBC binding (less than 5% relative to HA wt; marked as +−−). It is evident from the data that most of the mutations that involve replacement of residues of similar size had little effect on the ability to bind RBCs and that the reduction of the binding is proportional to the size difference between the amino acids of HA wt and the mutant. Our theoretical explanation is based on this observation.

4.2. Calculations

We used Eqs. (1) and (3) to calculate $\Delta\Delta G_{stab}$ as described in Computational methods. The results are presented in Table 1. The table depicts a good inverse correlation between the measured RBC binding and the calculated stability free energy of HA in its metastable state N; strong binding is correlated with small $\Delta\Delta G_{stab}$, while weak binding is correlated with large $\Delta\Delta G_{stab}$. To visualize the results and to facilitate quantitative comparison of the experimental data to the calculations, we processed the experimental data to fit a presentation as a diagram. The calculated values span a free energy range of 16.4−(−4.1)=20.5 kcal/mol, while the experimental data is reported in terms of four levels of binding: (+++), (++−), (+/−) and (+−−) that presumably correlate with the same free energy range. Thus, we scaled the calculated data to the experiments by fitting the extreme values of the calculations and measurements, i.e., −4.1 kcal/mol to (+++) and 16.4 kcal/mol to (+−−). The correlation implies that the "measured" free energy difference between each of the four levels is 20.5/4=5.1 kcal/mol, and thus the four levels are as follows: (+++) corresponds to the free energy range −4.1–1 kcal/mol, (++−) corresponds to the range 1–6.1 kcal/mol, (+/−) corresponds to 6.1–11.3 kcal/mol and (+−−) to 11.3–16.4 kcal/mol. The results of the scaling procedure are listed in Table 1 and are plotted in Fig. 5.

The chart in Fig. 5 shows the measured binding of the HA mutants relative to the wild-type compared to the calculated relative stability free energy of HA in its metastable form N. The mutations are plotted in decreasing order of the experimental binding index from (+++) to (+−−) and the figure shows the overall agreement between the

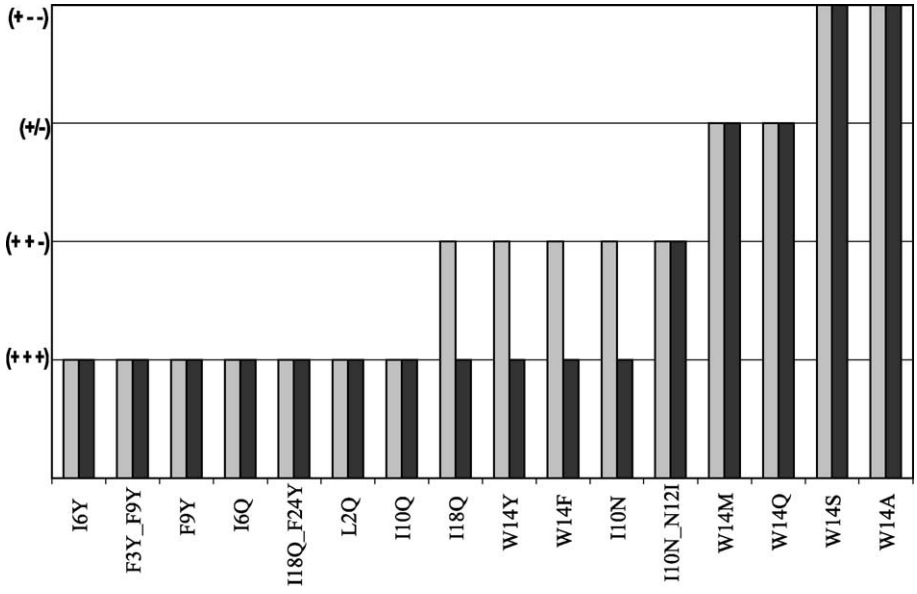

Fig. 5. The calculated stability (Fig. 2) and the measured R18-RBC binding of the HA mutants. The black and gray columns represent the experimental results and the calculations, respectively. The values are taken from Table 1. See text for details.

measurements and calculations over the entire range. Very good agreement is observed for 12 out of the 16 mutants that we have tested and the discrepancy between the experimental data and the calculations for the four other mutations does not exceed one level.

One-level deviations between measurements and calculations are observed for four single mutants: I18Q, W14Y, W14F and I10N. In all of these cases, the calculated value exceeds the measured value, presumably because of the oversimplified computational scheme that we used. This issue is discussed below.

5. Discussion

We carried out a mutagenesis study to explore whether the structure of the fusion peptide can alter HA binding to its cell-surface receptors at the distal site. Our main experimental observation is that some of the mutations reduced the binding ability, even though the fusion peptide and the receptor-binding site are about 100 Å away from each other and on two different HA subunits. The key observation here is that replacing residues with same-size residues had little or no effect on HA's cell-surface binding, while the replacement of large buried residues with small ones reduced the binding. The latter type of residue replacements is likely to lead to the creation of cavities in HA and to its destabilization. Since it is commonly found that reduced protein stability leads to reduced function [37], the simplest possible explanation for our experimental observation is that mutations that are associated with reduced stability of HA lead to reduced binding to cell-surface receptors.

Work by Sauter et al. [38,39] on pure molecules in solution indicated that native HA, low pH HA, and the isolated globular receptor-binding domain of HA all bind sialic acid with similar affinities. Thus, it might have been anticipated that it would be difficult to find mutations outside the receptor-binding domain itself that would compromise HA's function. However, the available experimental data suggest that the situation is much more complex for intact membrane-attached HA. For example, the exposure of virions or cells expressing HA to low pH, which presumably involves the shift of HA from the N to the F form, prior to providing them with a target membrane, was shown to inactivate the fusion activity of HA of the X:31 strain and to reduce its lateral mobility in the membrane [15–18].

The reason for the apparent conflict between studies of HA fragments in aqueous solutions vs. studies of the intact molecule in virions or cellular systems is unclear. One possible explanation is that pre-exposed fusion peptides in the latter experiments may stick to each other or to hydrophobic regions on HA or on the cell (or virion) membrane and may restrain HA's accessibility to its cell-surface receptors. In view of these findings (and regardless of the resolution of the conflict), we suggest here that the reduction in the stability of HA in the N conformation (Fig. 2a) may indeed impair the capacity of membrane-attached HA to bind to cell-surface receptors. The fact that, unlike most other proteins, the native (N) conformation of HA is metastable gives further support to our assumption, and the calculations of Table 1 and Fig. 5 consolidate it. In the following paragraphs, we discuss some limitations of the experimental methodology, the computational scheme, and the procedure used for relating the experimental and computational data.

Conducting experiments for accurately measuring the free energy of binding of HA to its sialic acid-containing receptors is difficult because these receptors comprise a heterogeneous population of many proteins and lipids; furthermore, these receptors are located at the cell surface and their availability and exact conformation may also depend on the membrane lipid environment. However, for the purpose of this study it was sufficient to get an estimate of the relative binding capacity of HA mutants compared to HA wt, which we did by measuring the binding of fluorescent-labeled RBCs to HA-expressing cells (see Experimental methods). The approximated experimental data thus obtained calls for a simple computational scheme of the type we used to interpret the data.

The method of choice for calculating the stability difference between HA mutants and HA wt (in their "N" conformation) is free energy perturbation using molecular dynamics simulations. The technique is well established and is the main computational tool for estimating the effects of mutations on binding and stability in biomolecules. It has been used to reproduce binding free energy differences between mutant and wild-type protein forms and yielded results in excellent agreement with experimental data [40]. Free energy calculations can, in principle, include all the free energy terms, contributions from internal energy and conformational entropy effects, as well as solvation free energy—provided that the simulations are carried out in water environment. Thus, they should be superior to our calculations that take into account only the nonpolar contribution to the solvation free energy (Eq. (3)).

However, molecular dynamics simulations for large systems, such as the HA trimer in water, are cpu time-demanding and the alternative simplified model that we chose provides a reasonable alternative—especially that the exact value of the free energy matters less than the relative value. It should be noted that the measured binding is only semi-quantitative; it is reported in levels relative to HA wt rather than as a free energy value.

External effects, such as the salt concentration, the pH and the temperature, are not included in our theoretical model and thus the approach is suitable only for the comparison of mutants at similar environment, e.g., physiological conditions as we used here.

One of the main difficulties of our study was to relate the estimate of the stability free energy in kcal/mol to the experimental data, reported in percent binding relative to HA wt. Since the trend matters more than the actual value in this study, we suggested the simplest possible relation, i.e.,

that the experimental data and the calculations are linearly proportional to each other, and our results are in agreement with this assumption. Another difficulty is that the actual value of the calculated stability free energy depends on the choice of the surface tension coefficient, γ, in Eq. (3). Typical γ values are between 0.02 and 0.05 kcal/(mol Å^2) [41] and we arbitrarily used a value of 0.0278 kcal/(mol Å^2) that has been derived from experimental data of transferring alkane molecules from cyclohexane to water [28]. However, it is noteworthy that the actual value of γ is not important for this study; our results show that the difference in the water accessible surface area between HA mutants and wt is linearly proportional to the measured difference in binding. The choice of γ determines only the range of the calculated values—about 20 kcal/mol in our case; had we chosen a smaller value of γ, the range to be obtained would be smaller but the proportion would not be altered.

Despite its limitations, our computational scheme provides estimates of changes in the binding-capability that agree well with the trend of the experimental data. This is presumably because we focused on the main contribution to protein stability and thus avoided the problem of subtracting very large values to estimate small changes in protein stability. The success of our scheme further supports the general view that the main contribution to the stability free energy is the nonpolar solvation term and that the other contributions probably cancel each other out approximately.

The approximated computational scheme was only used as a tool for interpreting the experimental data and our experimental and computational data suggests that distant mutations affect binding of HA to its receptors by changing the stability of the HA molecule in its metastable N conformation. This suggestion is further supported by proline scanning studies of HA. In these studies, we demonstrated that binding of the four HA mutants: A7P, N12P, M17P and Y22P to the cell-surface receptor is completely abolished. The mutation of each of these residues to proline presumably destabilizes HA in its metastable N conformation to a degree where almost all the mutant HA molecules shift to binding-incompetent conformations such as F, essentially eliminating the binding to cell-surface receptors. Proline mutations are likely to yield significant structural changes, i.e., the mutants' structures are likely to deviate significantly from HA wt, so that our computational scheme probably cannot be used as discussed above. Thus, we did not attempt to calculate the change in the stability free energy of the proline mutants.

The success of our model in the interpretation of the seemingly puzzling experimental data would be substantiated by demonstrating that the mutations affect HA stability. However, such studies are not feasible within the scope of the current work because they would require purification of all the HA mutants either as GST-fusion proteins in bacteria or in insect cells. Moreover, in view of the conflict between the results obtained by Sauter et al. [38,39] for purified/solubilized HAs and the data presented here for membrane-anchored intact HAs, even if such studies (on solubilized HAs) were performed, their merit might be questionable. In this context, it should be noted that HA is not homogeneously distributed in the membrane, but rather is associated with cholesterol- and sphingolipid-enriched raft domains [42,43]. This further complicates the comparison between studies on solubilized and membrane-attached HAs.

Acknowledgements

T.D. was a joint graduate student of Y.I.H. and Judith M. White; the mutations were carried out in White's lab. We thank Debora Fass, Michael H. Hecht, Amnon Horowitz, Gabriel Kaufmann, Nathan Nelson and Ezra Yagil for helpful discussions. The research was supported by fellowships from the Wolfson and Alon Foundations to N.B-T. We are grateful to the Bioinformatics Unit of the George S. Wise Faculty of Life Sciences at Tel Aviv University for providing computation facilities.

References

[1] C.M. Carr, P.S. Kim, Cell 73 (1993) 823–832.
[2] C.M. Carr, P.S. Kim, Science 266 (1994) 234–236.
[3] J.J. Skehel, D.C. Wiley, Ann. Rev. Biochem. 69 (2000) 531–569.
[4] D.C. Wiley, J.J. Skehel, Ann. Rev. Biochem. 56 (1987) 365–394.
[5] J.J. Skehel, D.C. Wiley, Cell 95 (1998) 871–874.
[6] T. Stegmann, A. Heleius, in: J. Bentz (Ed.), Viral Fusion Mechanisms, CRC Press, Boca Raton, 1993, pp. 89–111.
[7] J. Chen, K.H. Lee, D.A. Steinhauer, D.J. Stevens, J.J. Skehel, D.C. Wiley, Cell 95 (1998) 409–417.
[8] I.A. Wilson, J.J. Skehel, D.C. Wiley, Nature 289 (1981) 366–373.
[9] W.I. Weis, A.T. Brunger, J.J. Skehel, D.C. Wiley, J. Mol. Biol. 212 (1990) 737–761.
[10] P.A. Bullough, F.M. Hughson, J.J. Skehel, D.C. Wiley, Nature 371 (1994) 37–43.
[11] T. Korte, K. Ludwig, F.P. Booy, R. Blumenthal, A. Herrmann, J. Virol. 73 (1999) 4567–4574.
[12] C.M. Carr, C. Chaudhry, P.S. Kim, Proc. Natl. Acad. Sci. U. S. A. 94 (1997) 14306–14313.
[13] L.R. Hoffman, I.D. Kuntz, J.M. White, J. Virol. 71 (1997) 8808–8820.
[14] H. Qiao, S.L. Pelletier, L. Hoffman, J. Hacker, R.T. Armstrong, J.M. White, J. Cell Biol. 141 (1998) 1335–1347.
[15] O. Gutman, T. Danieli, J.M. White, Y.I. Henis, Biochemistry 32 (1993) 101–106.
[16] P.R. Junankar, R.J. Cherry, Biochim. Biophys. Acta 854 (1986) 198–206.
[17] A. Puri, F.P. Booy, R.W. Doms, J.M. White, R. Blumenthal, J. Virol. 64 (1990) 3824–3832.
[18] S.B. Sato, K. Kawasaki, S. Ohnishi, Proc. Natl. Acad. Sci. U. S. A. 80 (1983) 3153–3157.
[19] D. Eisenberg, A.D. McLachlan, Nature 319 (1986) 199–203.
[20] B. Honig, K. Sharp, A.S. Yang, J. Phys. Chem. 97 (1993) 1101–1109.
[21] B. Honig, A. Nicholls, Science 268 (1995) 1144–1149.
[22] J.T. Kellis Jr., K. Nyberg, D. Sali, A.R. Fersht, Nature 333 (1988) 784–786.
[23] J. Kyte, R.F. Doolittle, J. Mol. Biol. 157 (1982) 105–132.
[24] J.A. McCammon, Curr. Opin. Struct. Biol. 8 (1998) 245–249.
[25] A. Warshel, Computer Modeling of Chemical Reactions in Enzymes and Solutions, Wiley, New York, 1991.

[26] K. Yue, K.A. Dill, Protein Sci. 5 (1996) 254–261.
[27] Y. Nozaki, C. Tanford, J. Biol. Chem. 246 (1971) 2211–2217.
[28] D. Sitkoff, N. Ben-Tal, B. Honig, J. Phys. Chem. 100 (1996) 2744–2752.
[29] S.A. Sridharan, A. Nicholls, B. Honig, Biophys. J. 61 (1992) A174.
[30] A. Shrake, J.A. Rupley, J. Mol. Biol. 79 (1973) 351–371.
[31] T.A. Kunkel, J.D. Roberts, R.A. Zakour, Methods Enzymol. 154 (1987) 367–382.
[32] G.W. Kemble, T. Danieli, J.M. White, Cell 76 (1994) 383–391.
[33] G.W. Kemble, D.L. Bodian, J. Rose, I.A. Wilson, J.M. White, J. Virol. 66 (1992) 4940–4950.
[34] T. Danieli, S.L. Pelletier, Y.I. Henis, J.M. White, J. Cell Biol. 133 (1996) 559–569.
[35] R.S. Daniels, A.R. Douglas, J.J. Skehel, D.C. Wiley, J. Gen. Virol. 64 (1983) 1657–1662.
[36] E. Fire, C.M. Brown, M.G. Roth, Y.I. Henis, N.O. Petersen, J. Biol. Chem. 272 (1997) 29538–29545.
[37] E. Fersht, Structure and Mechanism in Protein Science, Freeman, New York, 1999.
[38] N.K. Sauter, M.D. Bednarski, B.A. Wurzburg, J.E. Hanson, G.M. Whitesides, J.J. Skehel, D.C. Wiley, Biochemistry 28 (1989) 8388–8396.
[39] N.K. Sauter, J.E. Hanson, G.D. Glick, J.H. Brown, R.L. Crowther, S.J. Park, J.J. Skehel, D.C. Wiley, Biochemistry 31 (1992) 9609–9621.
[40] P. Kollman, Chem. Rev. 93 (1993) 2395–2417.
[41] K.A. Sharp, A. Nicholls, R.F. Fine, B. Honig, Science 252 (1991) 106–109.
[42] K.A. Melkonian, A.G. Ostermeyer, J.Z. Chen, M.G. Roth, D.A. Brown, J. Biol. Chem. 274 (1999) 3910–3917.
[43] P. Scheiffele, M.G. Roth, K. Simons, EMBO J. 16 (1997) 5501–5508.